

# Single-Measurement Excitation/Emission Matrix Spectrofluorometer for Determination of Hydrocarbons in Ocean Water. 2. Calibration and Quantitation of Naphthalene and Styrene

Karl S. Booksh,<sup>†</sup> Allen R. Muroski, and M. L. Myrick\*

Department of Chemistry and Biochemistry, University of South Carolina, Columbia, South Carolina 29208

**An excitation/emission matrix imaging spectrofluorometer was employed for quantitation of two fluorescent compounds, naphthalene and styrene, contained in ocean water exposed to gasoline. Multidimensional parallel factor (PARAFAC) analysis models were used to resolve the naphthalene and styrene fluorescence spectra from a complex background signal and overlapping spectral interferences not included in the calibration set. Linearity was demonstrated over 2 orders of magnitude for determination of naphthalene with a detection limit of 8 parts per billion. Similarly, nearly 2 orders of magnitude of linearity was demonstrated in the determination of styrene with an 11 ppb limit of detection. Furthermore, the synthesis of the EEM spectrofluorometer and the PARAFAC analysis for unbiased prediction of naphthalene and styrene concentration in mixture samples containing uncalibrated spectral interferences was demonstrated.**

Dissolved hydrocarbons are present in nearly every natural water environment. Natural sources include humic acids, fulvic acids, and fish oils. Anthropogenic sources of contamination include fuel discharge from marine vessels, petroleum spills, and agricultural runoff of pesticides. For example, it is estimated that in 1988 alone 33.1 million pounds of benzene and 344.6 million pounds of toluene were released into the environment.<sup>1</sup> Obviously, analysis of natural waters for anthropogenic hydrocarbon contamination is important for both environmental health and regulatory reasons.

An ideal method for detecting and quantitating dissolved hydrocarbons would have a part-per-billion (ppb) detection limit, require no sample pretreatment, be fully selective to the analyte of interest, and perform rapid, in situ analysis with inexpensive, robust instrumentation. Where no single method meets all these criteria, chromatography multivariate detection systems have become accepted standards for environmental analysis for dissolved organic compounds.<sup>2,3</sup> GC- and HPLC-based systems are highly selective and robust and have a low detection limit for many environmentally relevant anthropogenic contaminants; however, analyte extraction and preconcentration are often required.<sup>2–5</sup> All

told, a single chromatographic analysis can require 1 h or longer. Sample turnaround time is often 2 or more days since field-portable units are expensive and lack the performance of laboratory analysis.

One alternative to chromatography is fluorescence spectroscopy.<sup>6,7</sup> Molecular fluorescence measurements can be rapidly and inexpensively performed in either an in situ or remote fashion.<sup>8–10</sup> Many environmentally important hydrocarbon contaminants are naturally fluorescent and detectable at the ppb level;<sup>11–13</sup> therefore, no sample preconcentration or derivatization is required. Unfortunately, the broad nature of fluorescence bands and the large number of fluorescent natural compounds prohibit complete analyte selectivity with both excitation- and emission-based measurements.

When univariate- or multivariate-based analysis of fluorescent data is employed, the lack of analyte selectivity hampers the ability to perform reliable and unbiased analyte quantitation. With univariate analysis (single-wavelength excitation or single-wavelength emission), the presence of an interfering fluorescent species biases the predicted analyte concentration. Worse, the presence of the interfering species cannot be detected by univariate spectroscopic techniques.<sup>14</sup> With multivariate analysis (single-wavelength excitation with multiple-wavelength emission, multiple-wavelength excitation with single-wavelength emission, and synchronous-scanning fluorometry), unbiased quantitation can be accomplished in the presence of spectral interferences; however, all spectrally interfering species must be included in the calibration set.<sup>14</sup> If an uncalibrated spectroscopic interferent is included in a predictive sample, the predicted analyte concentration will be biased. Fortunately, the presence of an uncalibrated interferent can be detected by multivariate spectroscopic techniques.<sup>15</sup> Multivariate fluorometry can also be coupled with chromatography or titration to estimate the intrinsic profiles of overlapping

(4) Volmer, D.; Levens, K.; Wuensch, G. *J. Chromatogr.* **1994**, *660*, 231–248.

(5) Butlerman, A. J.; Vreuls, J. J.; Ghijzen, R. T.; Brinkman, U. A. T. *J. High Resolut. Chromatogr.* **1993**, *16*, 397–403.

(6) Kucklick, J. R.; Bidleman, T. F. *Mar. Environ. Res.* **1993**, *37*, 63–78.

(7) Vilchez, J. S.; del Olmo, M.; Avidad, R.; Capitan-Vallvey, L. F. *Analyst* **1994**, *119*, 1215–1219.

(8) Taylor, T. A.; Jarvis, G. B.; Xu, H.; Bevilacqua, A. C.; Kenny, J. E. *Anal. Instrum.* **1993**, *21*, 141–162.

(9) Panne, U.; Niessner, R. *Sens. Actuators, B* **1993**, *13*, 288–292.

(10) Henderson-Kinney, A.; Kenny, J. E. *Spectroscopy* **1995**, *10* (7), 32–38.

(11) Files, L. A.; Winefordner, J. A. *J. Agric. Food Chem.* **1987**, *35*, 471–474.

(12) Rodriguez, J. J. S.; Garcia, J. H.; Suarez, M. M. B.; Martin-Lazaro, A. B. *Analyst* **1993**, *118*, 917–921.

(13) Myrick, M. L.; Muroski, A. R.; Groner, M., submitted to *Mar. Pollut. Bull.*

(14) Sanchez, E.; Kowalski, B. R. *J. Chemom.* **1988**, *2*, 247–263.

(15) Gemperline, P. J. *J. Chemom.* **1989**, *3*, 549–568.

<sup>†</sup> Present address: Department of Chemistry and Biochemistry, Arizona State University, Tempe, AZ 85287.

(1) McGrath, E. M.; Booksh, K. S.; Breen, J. J. In *Process Analytical Chemistry*; McLennan, F., Kowalski, B. R., Eds.; Chapman-Hall: New York, 1995.

(2) Sherma, J. *Anal. Chem.* **1995**, *67*, 1R–20R.

(3) Clement, R. E.; Eiceman, G. A.; Koester, C. J. *Anal. Chem.* **1995**, *67*, 221R–255R.

fluorescent species.<sup>16,17</sup> While this method for spectral deconvolution has met with some success, the implicit assumption of "one unique measurement for every species" required to derive a unique solution is seldom valid.

Collection of an entire excitation/emission matrix (EEM) fluorescence spectrum for every sample analyzed reduces the concerns derived from the inability to collect instrumentally resolved analyte spectra. With EEM fluorescence, mathematical, not physical or spectral, separation of analytes can be achieved.<sup>18</sup> This separation permits unbiased analyte quantitation in the presence of uncalibrated, spectroscopically interfering species.<sup>18</sup> Multidimensional mathematical and statistical spectral deconvolution methods have been combined with tunable laser-based EEM fluorometers to extract quantitative<sup>19,20</sup> and qualitative<sup>20,21</sup> information.

Presented here is the symbiosis of an arc lamp-based imaging EEM fluorometer and a multidimensional spectral deconvolution technique. In the previous paper, it was demonstrated that multidimensional spectral deconvolution can separate the intrinsic fluorescence of each sample from a complex background.<sup>22</sup> In this paper, it is demonstrated that unbiased analyte quantitation can be accomplished in the presence of varying background signals and uncalibrated spectroscopic interferents. The abilities of the EEM system are demonstrated for the quantitation of naphthalene in ocean water/gasoline mixtures and styrene in ocean water/toluene mixtures.

## EXPERIMENTAL SECTION

**Instrumentation.** A spectrofluorometer was constructed for the purpose of collecting a practical EEM of analytes at ppb concentrations in less than 1 min. This system employed an Oriol Model 66021 high-pressure 1000-W Hg(Xe) arc lamp and two imaging spectrographs to produce a spatially resolved EEM. The EEM fluorescence spectrum of each sample was recorded by analog-to-digital conversion of the output from a Santa Barbara Instrument Group Model ST-6 thermoelectrically cooled CCD camera. Further details of the EEM spectrofluorometer are contained in the previous paper.<sup>22</sup>

Solutions of naphthalene/gasoline in ocean water and styrene/gasoline in ocean water were prepared by combining standard solutions of naphthalene and styrene in this matrix with a solution of gasoline in ocean water. The solutions of naphthalene in ocean water and styrene in ocean water were prepared as described in the first paper. The gasoline/ocean water solution was produced by exposing 2 mL of Shell "premium" 93-octane gasoline to 1 L of ocean water for 24 h in a separatory funnel. The aqueous layer of this combination was then drained into a separate glass container for storage. A solution of toluene at an unknown concentration in ocean water as an uncalibrated interferent for styrene was prepared by exposing 100 mL of water to 1 mL of

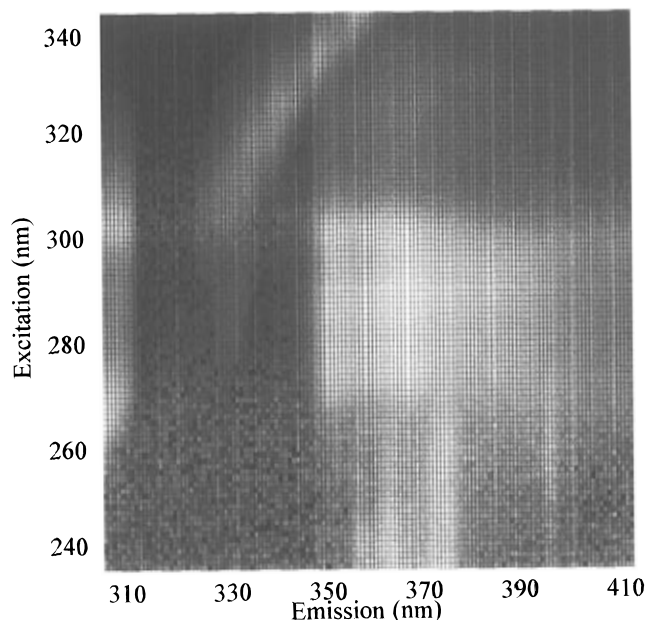


Figure 1. Excitation/emission spectrum (corrected for sample irradiance) of 857 ppb naphthalene in a gasoline/ocean water matrix. The intense elastic scattering is evident in the upper left-hand quadrant.

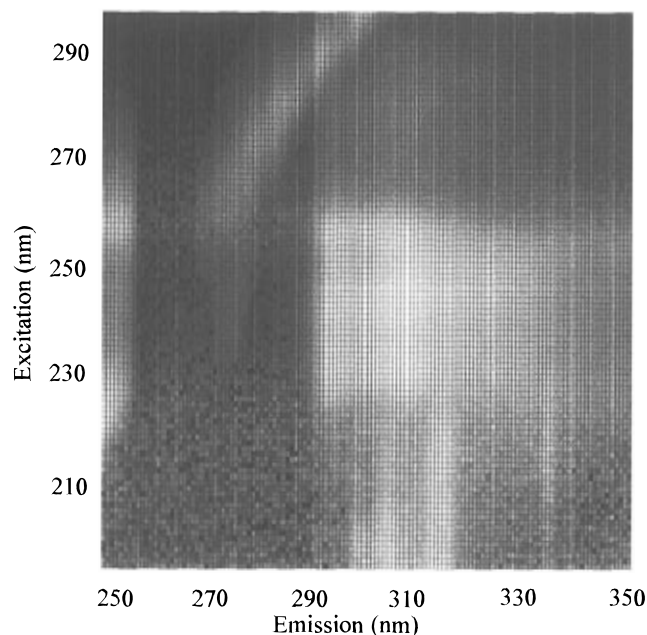


Figure 2. Excitation/emission matrix (corrected for sample irradiance) of 750 ppb styrene in an ocean water matrix.

toluene (99+%, Aldrich) for 24 h. Solutions ranging from 0 to 75 ppb styrene but unknown toluene concentration in ocean water were produced by combining aliquots of both hydrocarbon/ocean water solutions.

Figure 1 presents the EEM of 857 ppb naphthalene in ocean water that had been spiked with the aqueous gasoline extract. Integration of the total fluorescence in the spectral region of interest indicates that the background, resulting from a combination of instrumental factors and the presence of gasoline hydrocarbons, is 48% of the total signal in this spectral region. Figure 2 is an EEM of 750 ppb styrene in ocean water.

**Data Pretreatment.** The EEMs were collected and stored in "low-resolution" mode with the CCD operating software. This

- (16) Silva, C. S. P. S. O.; da Silva, J. C. G. E.; Machado, A. A. S. C. *Appl. Spectrosc.* **1994**, *48*, 363–372.
- (17) Langford, C. H.; Cook, R. L. *Analyst* **1995**, *120*, 591–596.
- (18) Sanchez, E.; Kowalski, B. R. *J. Chemom.* **1988**, *2*, 265–280.
- (19) Ferreira, M. M. C.; Brandes, M. L.; Ferreira, I. M. C.; Booksh, K. S.; Dolowy, W. C.; Gouterman, M.; Kowalski, B. R. *Appl. Spectrosc.* **1995**, *49*, 1317–1325.
- (20) Burdick, D. S.; Tu, X. M.; McGown, L. B.; Millican, D. W. *J. Chemom.* **1990**, *4*, 15–28.
- (21) Ho, C.-N.; Christian, G. D.; Davidson, E. R. *Anal. Chem.* **1978**, *50*, 1108–1113.
- (22) Muroski, A. R.; Booksh, K. S.; Myrick, M. L. *Anal. Chem.* **1996**, *68*, 3534–3538 (preceding paper in this issue).

mode bins three horizontal and two vertical pixels and reduces the time and space required for digitizing, downloading, and storing the images while improving the signal-to-noise ratio of each image. Each  $250 \times 121$  element image was converted from a double-precision SBIG file<sup>23</sup> to a double-precision ASCII file by an internally written C++ program. Each image was dark count subtracted, normalized to correct for the wavelength dependence of the sample irradiance, and compressed to a  $60 \times 90$  element matrix that spanned approximately 105 nm in the excitation domain and 115 nm in the emission domain. All postconversion data treatment were performed in the Matlab (MathWorks Inc., Natick MA) operating environment on Gateway P5-90 (Gateway2000, E. Sioux Falls, SD) personal computers. Further details of the data compression and pretreatment are discussed in the first paper in this series.<sup>22</sup>

**Multidimensional Models.** Discussion of multidimensional data structures,<sup>24</sup> and algorithms,<sup>25–27</sup> benefits,<sup>18,28</sup> dangers,<sup>29</sup> and applications<sup>19–21,30–32</sup> associated with multidimensional analysis are well documented, and an abbreviated version of multidimensional spectral resolution is provided in the previous paper.<sup>22</sup> In this application, the collection of EEMs,  $\mathbf{R}$ , consisting of calibration samples and unknown mixture samples forms a three-dimensional data structure dimensioned  $I$  excitation wavelengths by  $J$  emission wavelengths by  $K$  samples. Provided neither the excitation spectra, emission spectra, nor relative concentrations of the constituent species in the collection of EEMs are collinear, this cube of data can be uniquely decomposed via a  $N$  factor parallel factor analysis (PARAFAC) model,<sup>33</sup>

$$R_{i,j,k} = \sum \hat{X}_{i,n} \hat{Y}_{j,n} \hat{Z}_{k,n} + E_{i,j,k} \quad (1)$$

into the estimates of the underlying excitation ( $\hat{\mathbf{X}}$ ), emission ( $\hat{\mathbf{Y}}$ ), and relative resolved spectral intensity ( $\hat{\mathbf{Z}}$ ) profiles where  $N$  is the number of spectrally detectable species in the EEM collection. Here  $\hat{\mathbf{X}}$  is a  $I \times N$  matrix and  $\hat{\mathbf{Y}}$  is a  $J \times N$  matrix, where each column corresponds to the estimated excitation and emission fluorescence profile, respectively, of one of the  $N$  detectable species in the collection of samples. Since the columns of  $\hat{\mathbf{X}}$  and  $\hat{\mathbf{Y}}$  are scaled to unit area, the elements of  $\hat{\mathbf{Z}}$  contain the relative spectral intensities associated with the  $K$  samples for each of the  $N$  compounds. It is assumed that there is a linear relation between spectral intensity and concentration. The tensor  $\mathbf{E}$  is the collection of residual errors associated with the model.

There are three important issues that must be noted about the PARAFAC decomposition. First, the success of the model is dependent on the choice of the number of factors,  $N$ . If  $N$  is less than the number of distinct compounds, the errors associated with

the PARAFAC model will be large, the estimated excitation and emission profiles will not conform to reality, and calibration based on the relative resolved spectral intensities will be inaccurate. If the choice of  $N$  is greater than the number of distinct compounds, the PARAFAC model will be forced to describe minor sources of systematic instrumental errors; this often results in estimates of the excitation and emission profiles that are not physically meaningful and also inaccurate calibration based on the relative spectral intensities. Second, a spectrally distinct component could be nonchemical in nature, e.g. the background due to stray excitation energy. Finally, the capability to perform accurate quantitation in the presence of compounds not included in the calibration set is derived from the simultaneous decomposition of the calibration and unknown samples by the PARAFAC model. By this method the entire analyte spectrum can be uniquely resolved from the unknown sample's EEM.

For this application, an alternating least-squares-based algorithm was chosen for decomposition of the collection of EEMs into intrinsic factors. The theory behind this type of algorithm has been presented by Kroonenberg,<sup>27,33</sup> and is covered in other applications-driven manuscripts.<sup>30,32</sup> Details regarding optimal convergence criteria, model validation, and pertinence of the PARAFAC model to EEM data are contained in the previous paper.<sup>22</sup>

## RESULTS AND DISCUSSION

**Naphthalene Calibration and Quantitation.** The collection of 11 naphthalene/ocean water and background EEMs were decomposed via a two-factor PARAFAC model in the form of eq 1. The decomposition produced estimates of the excitation and emission profiles of naphthalene and the background as well as estimates of the relative naphthalene and background intensities among the samples. Incorporating a third factor did not significantly decrease the error of fit for the model to the EEMs and resulted in "negative" excitation and emission profile estimates. Similarly, inclusion of the 12 aqueous gasoline samples in the collection necessitated a third factor for optimal decomposition to model the fluorescence spectrum of the gasoline.

Two calibration curves for naphthalene in ocean water were constructed as a plot of the predicted relative concentration from the two-factor model versus the known naphthalene addition in each sample. The ability of the PARAFAC model to separate the naphthalene fluorescence from the background was discussed in the previous paper.<sup>22</sup> The factor that corresponds to naphthalene has a 2.6 ppb standard deviation (5 df) of the blank which is equivalent to a limit of determination of eight ppb ( $3\sigma$ ). Hence, the measured linear dynamic range for naphthalene extends over 2 orders of magnitude (8–2000 ppb). The root-mean-squared error of prediction for all 19 standards is 47.3 ppb; individual errors associated with each nonblank are included in Table 1.

Three of the naphthalene/ocean water standards (666, 800, and 1000 ppb naphthalene) deviate from a linear relationship between the estimated relative concentration and the reported concentration of added naphthalene. In Table 1, it is further seen that two of these three standards have high prediction errors. Removal of all three standards before regression reduces the overall root-mean-squared error to 19.2 ppb. All three removed standards are outliers at the 99% confidence level based on the new regression. Hence, 19 ppb might be a more accurate measure of the precision associated with analysis.

(23) *Software Application Note*, Santa Barbara Instrument Group, Santa Barbara, CA.

(24) Esbensen, K. H.; Wold, S.; Geladi, P. *J. Chemom.* **1988**, *3*, 33–48.

(25) Sanchez, E.; Kowalski, B. R. *J. Chemom.* **1990**, *4*, 29–46.

(26) Ohman, J.; Geladi, P.; Wold, S. *J. Chemom.* **1990**, *4*, 79.

(27) Kroonenberg, P. *Three Mode Principal Component Analysis*, DSWO Press: Leiden, The Netherlands, 1983.

(28) Booksh, K. S.; Kowalski, B. R. *Anal. Chem.* **1994**, *66*, 782A–791A.

(29) Smilde, A. K. *Chemom. Lab.* **1991**, *15*, 143–157.

(30) Gemperline, P. J.; Miller, K. H.; West, T. L.; Weinstein, J. E.; Hamilton, J. G.; Bray, J. T. *Anal. Chem.* **1992**, *64*, 523A–531A.

(31) Booksh, K. S.; Henshaw, J. M.; Burgess, L. W.; Kowalski, B. R. *J. Chemom.* **1995**, *9*, 263–282.

(32) Ross, R.; Lee, C.-H.; Davis, C.; Ezzeddine, B.; Fayyad, E.; Leugans, S. *Biochim. Biophys. Acta* **1991**, *1056*, 317–320.

(33) Kroonenberg, P.; deLeeuw, J. *Psychometrika* **1980**, *45*, 69–97.

Table 1. Errors in Self-Prediction for Naphthalene Standards Associated with a Two-Factor PARAFAC Model Applied to Only the Naphthalene/Ocean Water Standards and a Three-Factor PARAFAC Model Applied to Both the Naphthalene/Ocean Water Standards and the Naphthalene/Gasoline/Ocean Water Samples

naphthalene added (ppb)	prediction error (ppb)	
	2 factor	3 factor
28	-9.5 (4.0) <sup>a</sup>	-10.8 (2.6) <sup>a</sup>
28	-13.3 (-0.1)	-14.3 (-1.0)
56	-6.7 (7.4)	-4.1 (10.0)
84	-11.5 (3.1)	-12.8 (1.8)
110	-18.3 (-3.2)	-17.5 (-2.5)
286	-14.0 (4.7)	-16.0 (2.7)
571	-30.2 (-5.9)	-31.9 (-7.6)
666	78.3	77.7
800	113.0	112.2
1000	40.8	42.7
1333	-90.3 (-51.5)	-91.0 (-52.0)
2000	-18.9 (35.1)	-18.8 (36.2)
RMSE <sup>b</sup>	47.2 (19.2)	47.3 (19.7)

<sup>a</sup> Errors derived after discarding the 666, 800, and 1000 ppb naphthalene/ocean water standards. <sup>b</sup> Including blanks.

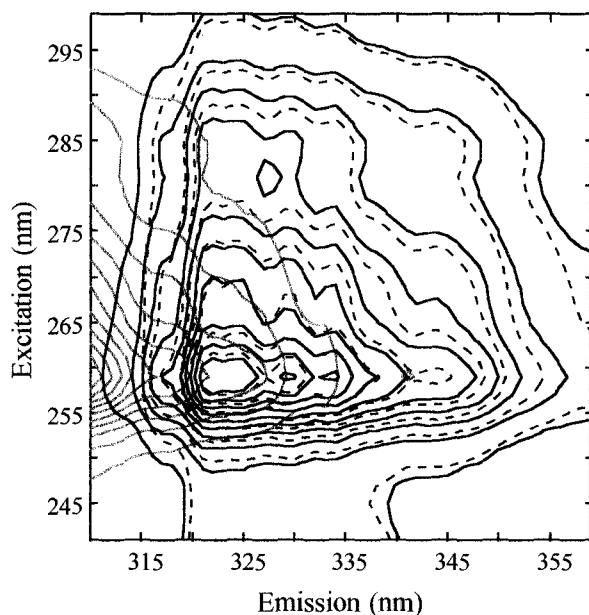


Figure 3. Resolved excitation/emission matrix spectra of naphthalene from two-factor PARAFAC model applied to the naphthalene/ocean water samples (dashed lines) and naphthalene (black) and gasoline (gray) from a three-factor PARAFAC model applied to the naphthalene/gasoline/ocean water samples.

Twelve samples containing a significant concentration of an aqueous gasoline extract were employed as unknown samples for naphthalene determination. Estimates of the excitation and emission spectra and relative concentrations for the constituent species were simultaneously determined for the naphthalene/ocean water and naphthalene/gasoline/ocean water samples with a three-factor PARAFAC model. Figure 3 compares the resolved naphthalene EEM spectrum from deconvolution of the naphthalene/ocean water samples (dashed) and naphthalene/gasoline/ocean water samples (black). Note that the presence of overlapping gasoline (gray) and background spectra does not affect these EEM estimations. Comparison of the second and third columns in Table 1 show that inclusion of gasoline-laden unknown samples in the collection of EEMs does not degrade the

Table 2. Figures of Merit for Prediction of Naphthalene in Naphthalene/Gasoline/Ocean Water Samples Based on the Calibration Derived from Naphthalene/Ocean Water Standards

naphthalene added <sup>a</sup> (ppb)	prediction error (ppb)	std dev <sup>b</sup> (ppb)
0 (3)	-9.7	26.7
143 (1)	-18.1	43.9
286 (1)	16.2	43.6
571 (2)	10.0	33.1
857 (2)	-3.2	34.3
1143 (1)	-90.5	47.3
1714 (2)	-107.9	42.3

<sup>a</sup> Numbers in parentheses indicate number of samples used for mean. <sup>b</sup> Derived from the estimated standard deviation of regression based on fit to sample concentration.<sup>34</sup>

quality of the calibration curve formed by the naphthalene/ocean water standards, provided an extra factor is included in eq 1 to account for the aqueous gasoline extract. With both the two-factor naphthalene/ocean water model and three-factor naphthalene/gasoline/ocean water models, the root-mean-squared error of prediction is approximately 47 ppb for the standards, and the 666, 800, and 1000 ppb standards deviate from linearity on the calibration curve. Removal of the three questionable samples drops the root-mean-squared error of prediction to less than 20 ppb in both cases.

Of greater importance, the ability of the spectrofluorometer to accurately quantitate analytes in the presence of large background signals and uncalibrated interferents is evident in the determination of naphthalene in gasoline/ocean water samples. Analysis of these samples shows the concentration of naphthalene to be 3 ppm ( $\sigma = 0.26$  ppm) in the undiluted gasoline extract. Therefore, dilution of a 0.5-mL gasoline extract to 4 mL corresponds to an intrinsic 306 ppb ( $\sigma = 32$  ppb) background naphthalene concentration in a naphthalene/gasoline/ocean water sample. Table 2 presents the error in recovered naphthalene concentration from the naphthalene-spiked gasoline/ocean water samples. For the samples ranging from 0 to 857 ppb naphthalene added, the mean error of recovery is comparable to the errors associated with naphthalene quantitation in the standards. The standard deviation associated with each prediction is derived from the standard deviation,  $\sigma$ , of the standards about the regression.<sup>34</sup> The value of this standard deviation is quite large since the conservative 17-sample model was employed to estimate quantitation reliability. Although the 1143 and 1714 ppb naphthalene additions are biased low in the predicted naphthalene concentration, note that these samples actually contain 1400 and 2000 ppb naphthalene, respectively, along with a substantial quantity of other dissolved hydrocarbons. The relatively large prediction errors associated with these samples can be justified by considering the samples' location at the extreme end of the calibration set, where the density of standards is low, and also considering that the high concentration of other dissolved hydrocarbons may limit the solubility of naphthalene.

**Styrene Calibration and Quantitation.** The EEM spectra from the styrene/ocean water standards, as the naphthalene/ocean water standard EEMs, were decomposed based on a two-

(34) Skoog, D. A.; West, D. M. *Analytical Chemistry, An Introduction*; 4th ed.; Saunders College Publishing: Philadelphia, 1986.

factor PARAFAC model of eq 1 to resolve the analyte fluorescence from the instrumental background. A plot of the relative resolved styrene intensity,  $\hat{Z}$ , against known styrene concentration is linear over the tested range of 50–1000 ppb styrene. There appears to be a slight nonlinearity between the blanks and the 50 ppb samples. This could be a result of adsorption of the diffuse styrene in the ocean water on the sides of the cuvette.

Regression of the 25 predicted relative resolved intensities against the known styrene concentration results in a mean-squared error of calibration of 26.9 ppb styrene. The standard deviation of the estimated styrene concentration for the seven instrumental blanks is 4.4 ppb. It was noted that two of the blanks had a substantially higher predicted styrene concentration than the other six. Discarding these two samples reduces the standard deviation to 0.65 ppb styrene. This corresponds to a calculated detection limit of 13 ppb and an optimistic detection limit of two ppb styrene.

Noting that the largest calibration errors occurred at higher styrene concentrations, and that most environmental applications would require detection of concentrations of less than 300 ppb styrene, the PARAFAC resolution and calibration was repeated on just the samples with 300 ppb styrene or less. For these 16 samples and blanks, the root-mean-squared error of regression over this reduced concentration range is only 6.0 ppb styrene with a 3.8 ppb styrene standard deviation of the seven blanks. The corresponding 11 ppb detection limit is comparable to the 13 ppb detection limit derived from resolution and calibration of expanded styrene/ocean water collection of samples. Of note is the fact that the relative spectral intensity of the average instrumental background is comparable to the spectral intensity of 300 ppb styrene.

The styrene/ocean water standards in the 0–300 ppb range were employed for deconvolution and calibration with the styrene/toluene/ocean water samples. A three-factor PARAFAC model was found to optimally resolve the styrene EEM spectrum from the background for these standards. A two-factor PARAFAC model resulted in an unacceptably large root-mean-squared error in regression of 10.5 ppb, compared to 6.0 ppb for the two-factor model applied to the styrene standards and the nearly identical 6.0 ppb for the three-factor PARAFAC model applied the entire collection of styrene/ocean water standards and the styrene/toluene/ocean water samples. Application of a four-factor PARAFAC model resulted in unrealistic estimates of the excitation and emission profiles. Linearity, again, is demonstrated between 50 and 300 ppb styrene; the inclusion of the toluene does not degrade formation of the calibration when an additional factor is included in the PARAFAC model.

The styrene concentration in the styrene/toluene/ocean water samples cannot be compared directly to the styrene concentration in the styrene/ocean water standards since the styrene stock solution partially polymerized between interrogating the mixtures and the standards. Hence, the reported styrene concentrations should be regarded as internally relative, not absolute values; however, the validity of the instrumental method and data analysis technique can still be demonstrated by simultaneously decomposing the mixtures and the standards via eq 1. If the PARAFAC model were incapable of resolving the styrene spectrum from the toluene and background signals, the random toluene concentration in the mixtures would destroy the linear relationship between the resolved relative styrene intensity and the reported styrene concentration.

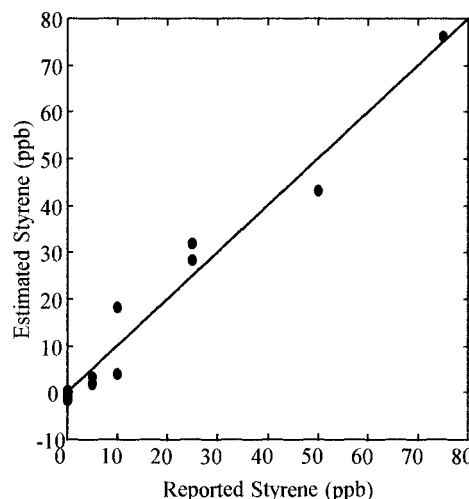


Figure 4. Estimated versus reported styrene concentrations derived from a three-factor PARAFAC model applied to analysis of styrene/toluene/ocean water mixtures.

Table 3. Figures of Merit for Prediction of Styrene in Styrene/Toluene/Ocean Water Samples

styrene <sup>a</sup> (ppb)	prediction error (ppb)	std dev <sup>b</sup> (ppb)
0 (6)	0.3	1.6
5 (2)	2.3	2.3
10 (2)	-1.1	2.3
25 (2)	-5.1	2.3
50 (1)	6.7	3.3
75 (1)	-1.1	3.8

<sup>a</sup> Numbers in parentheses indicate number of samples used for mean. <sup>b</sup> Derived from the estimated standard deviation of regression based on fit to sample concentration.<sup>34</sup>

That the styrene EEM spectrum can be resolved and an accurate calibration performed in the presence of toluene is evident in the plot of estimated versus reported styrene (Figure 4). A linear relation between the estimated and reported styrene concentration is clearly demonstrated. Table 3 presents the mean predicted styrene concentration and associated standard deviation derived from the regression.<sup>34</sup> There is no bias in the estimated concentrations as would be expected if the presence of toluene adversely affected the styrene calibration.

In fact, the linearity of the calibration and the standard deviation of the styrene blanks are significantly superior for the set of samples with toluene than the set of samples without toluene. There are two reasons to explain this disparity. Since the mixtures contain a large excess of toluene compared to styrene, the toluene out-competes the styrene for adsorption sites on the cuvette walls. Also, the styrene/ocean water standards were constructed from the partially polymerized styrene stock solution. The slope of the resolved relative styrene intensity versus reported styrene concentration is 25% less for the standards than for the mixtures. Therefore, variance in the resolved relative styrene intensities propagates as larger variance in the estimated styrene concentration for the set of standards than for the set of styrene/toluene/ocean water samples.

It is of further interest to investigate the resolved EEMs with and without toluene in the sample set. The ability to deconvolve the styrene EEM fluorescence spectrum from the overlapping background was discussed in the previous paper.<sup>22</sup> This background was shown to consist largely of horizontal and vertical

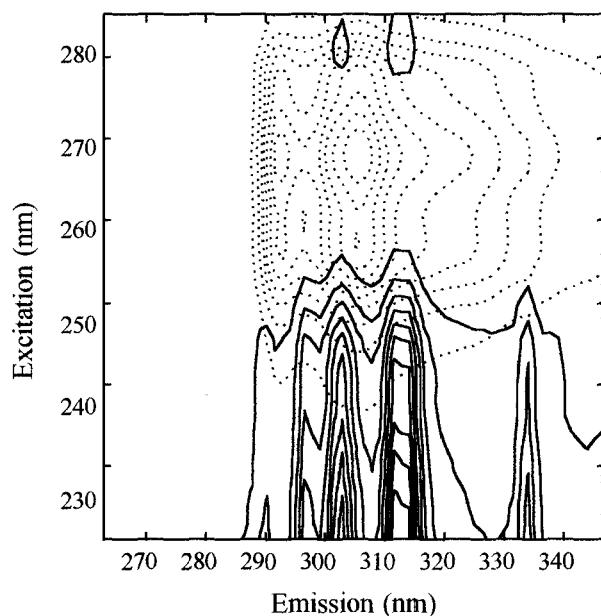


Figure 5. Resolved excitation/emission matrix spectra of styrene (dotted) and the background (solid) from a two-factor PARAFAC model applied to styrene/ocean water standards.

striations associated with Rayleigh scattering by solutes and Debye/Mie scattering by suspended particles. These scattering striations are especially intense where they correspond to mercury lamp lines. Note that since the dissolved analyte is directly responsible for a portion of the Rayleigh scattering, the proportion of the associated Rayleigh scattered light correlated with the analyte concentration will be indistinguishable from the analyte's fluorescence. Hence, these horizontal striations are embedded in the resolved EEM of the analyte. This is seen in the contour plot of the resolved EEMs of the styrene and scattering background for the two-factor PARAFAC model applied to the styrene/ocean water standards (Figure 5). The black contour lines correspond to the background while the dotted contour lines clearly correspond to the styrene.

Figure 6 presents the resolved EEM contour plots for styrene (dotted), background (solid), and the factor correlated with toluene concentration (dashed). This factor is not a model of the

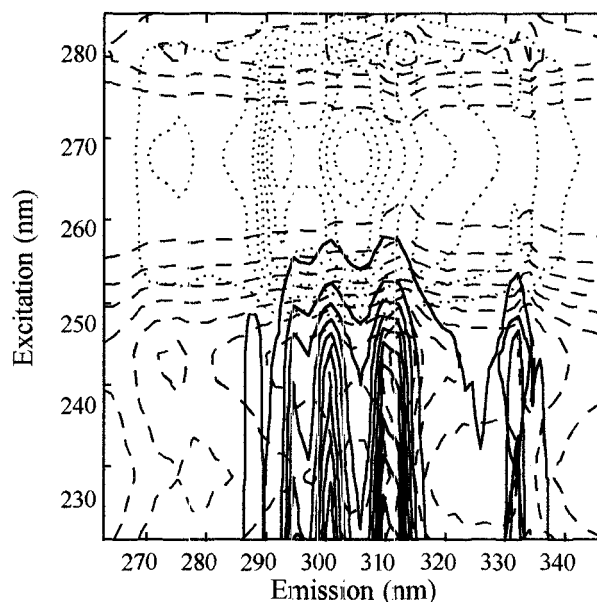


Figure 6. Resolved excitation/emission matrix spectra of styrene (dotted), toluene (dashed), and the background (solid) from a three-factor PARAFAC model applied to styrene/toluene/ocean water samples.

fluorescence spectrum of the toluene, but a model of the increased Rayleigh scattering correlated with variance in the toluene concentration. The 280-nm Hg lamp line can be distinguished clearly in this spectrum. The effects induced by the presence of toluene highlight two very important features of sample analysis with the EEM spectrofluorometer: nonfluorescent species can manifest themselves as spectral interferents, and these spectral interferents do not degrade accuracy or precision of determination when the proper number of factors is included in the PARAFAC model.

Received for review March 13, 1996. Accepted June 28, 1996.<sup>®</sup>

AC9602534

<sup>®</sup> Abstract published in *Advance ACS Abstracts*, August 1, 1996.